Electrically conducting nanofiltration membranes based on networked cellulose and carbon nanostructures

Farah Ejaz Ahmed[1], Boor Singh Lalia[1], Nidal Hilal[2] and Raed Hashaikeh[1]*

[1]Institute Center for Water Advanced Technology and Environmental Research (iWATER), Masdar Institute of Science and Technology, P.O. Box 54224, Abu Dhabi, United Arab Emirates

[2]Centre for Water Advanced Technologies and Environmental Research (CWATER),

College of Engineering, Swansea University, Swansea SA2 8PP, UK

*Corresponding author

Email: rhashaikeh@masdar.ac.ae

Phone: +971-28109152

Aug 2016

Abstract

Electrically enhanced fouling control is increasingly applied to membrane-based separation and requires conducting membranes with controlled properties. In this work, electrically conductive membranes based on networked cellulose (NC) and carbon nanostructures (CNS) were fabricated via vacuum filtration, followed by drying at 40 °C. The morphology, structure, mechanical and electrochemical properties of these NC-CNS membranes were characterized and compared with CNS membranes. The effect of incorporating NC on the electrocatalytic activity has been analyzed. It is found that networked cellulose helps to decrease the contact angle of water from 105 ° to 73°. It is also found that the improved surface hydrophilicity of CNS-NC membrane assists the regeneration of electrode surface during electrolysis process. Networked cellulose yields a more dense structure with the tensile strength exceeding ten times that of CNS alone. The compaction of pore structure via incorporation of NC translates into promising results with respect to nanofiltration of divalent ions, with a rejection efficiency of 60% for $MgSO_4$ and 47% for $CaCl_2$, while maintaining a high flux $\geq$ 100 L m^{-2} h^{-1}, making them suitable for pretreatment of RO feeds.

Keywords: Carbon nanostructures, cellulose, electrical conductivity, fouling, hydrophilic

1. Introduction

Membrane based water treatment plays a crucial role in obtaining potable water through reclamation of wastewater and seawater desalination. Membranes offer several advantages over other processes, as they are simple, do not require chemical additives and can be easily scaled up. Despite the rapid rise in the use of membrane processes, the most widely used polymeric membranes are susceptible to fouling, which increases energy costs for cleaning the membrane and often requires replacement as frequent cleaning deteriorate membrane quality with time. Recently, impregnation of electrically conductive material such as carbon nanotubes (CNTs) in polymeric membranes has led to the development of electrically enhanced fouling control through oxidation of foulants [1, 2] as well as gas bubble generation [3, 4]. CNT-based conductive membranes prevent fouling through several possible mechanisms including electrophoretic transport of foulants, direct oxidation, bubble generation, inherent antimicrobial properties of CNTs as well as bacterial detachment due to cathodic current [5]. This relatively new approach allows the non-destructive, energy efficient control of membrane fouling. However, the challenge is to develop membrane materials that are electrically conductive and electrocatalytically active without compromising their flux and selectivity.

Although electrically conductive membranes have been fabricated for simple filtration, only a few studies have focused on developing conductive membranes for pressure-driven processes such as ultrafiltration, nanofiltration and reverse osmosis [6-9]. These materials rely on CNT-polymer composites to maintain the selectivity and flux of polymeric membranes while enhancing their conductivity with CNTs. Despite progress in NF membrane materials, fouling mitigation to recover flux still largely relies on chemical cleaning techniques. However, common chemical cleaning agents such as caustic acid have been shown to alter NF membrane surface properties,

and in turn their separation efficiency [10]. Periodic electrolysis has previously been applied for successful flux recovery in carbon nanostructure membranes, through cathodic hydrogen bubble generation [4]. The aim of the current study is to attempt to control the pore size and surface characteristics of such conductive membranes to be suited to the separation of multivalent salts, in order to allow electrolytic cleaning to be used with NF.

Cellulose and cellulose-based derivatives are widely used as membrane materials for various separation processes. Cellulose is the world's most abundant natural raw material with several attractive properties, namely biodegradability, biocompatibility and excellent chemical stability. Through controlled dissolution in sulfuric acid followed by regeneration, native cellulose can be processed into a gel-like suspension known as networked cellulose (NC) [11]. NC has a more amorphous and more accessible structure than native cellulose and has previously been used to control the swelling of polyvinyl alcohol (PVA) RO membranes [12].

Carbon Nanostructures (CNS) consist of entangled and covalently bonded CNTs that are made through a scalable and low cost process by Applied Nanostructured Solutions (ANS), a subsidiary of Lockheed Martin (USA). CNS are structures of highly entangled CNTs that may share common walls. They are characterized by improved processability, high electrical conductivity and large surface area [13]. In our previous work, CNS were used to fabricate microfiltration membranes that worked successfully as electrically conductive self-cleaning membranes[4].

In this work, self-supporting NC/CNS membranes in which NC serves to enhance the mechanical properties and compact the pore structure while retaining high electrical conductivity have been developed. The novel material is characterized for morphology, structure and mechanical properties. The performance of this novel membrane material is studied with respect to

electrocatalytic activity and nanofiltration of divalent salts, in an attempt to identify its potential as a self-cleaning nanofiltration membrane.

2. Materials and Methods

Microcrystalline cellulose, Avicel PH 101 (Mw: 160 kDa–560 kDa), was purchased from FMC Biopolymer (USA). CNS (300 μm) was developed by Applied NanoStructured Solutions, LLC through a continuous chemical vapor deposition process [4, 14]. Ethanol (≥ 99%) and sulfuric acid (> 90%) were purchased from Sigma Aldrich. All materials were used as received.

2.1 Fabrication of NC/CNS membrane

Networked cellulose (NC) is prepared via acid hydrolysis of cellulose [11] with a Varian® dissolution system. Sulfuric acid (70% w/w concentration) was stabilized to 5 °C in the dissolution system using a water bath. 10g MCC was slowly added to 100 ml of sulfuric acid and mixed at 250 rpm for 20 minutes. Consequently, 10g CNS was also weighed and added to the cellulose solution and further stirred for 10 minutes. At this stage, ethanol at 5 °C was added to regenerate the cellulose. Acid was then removed by centrifugation of the resulting material at least three times. To ensure thorough removal of the acid, the resulting NC/CNS precipitate was dialyzed for three days, until the measured pH was about 6-7. The obtained black suspension was homogenized with a mechanical homogenizer (IKA-T25 ULTRA-TURRAX) to yield a uniform thick aqueous NC/CNS suspension.

The NC/CNS (1:1 w/w) suspension was diluted to 0.1 wt% before it was vacuum filtered through filter paper. The obtained NC/CNS membrane was dried under vacuum using the Huefer slab gel drier (model no. GD 2000) at 40 °C for 1 hour.

2.2 Membrane characterization

2.2.1 Morphology

The morphology of CNS and NC/CNS membranes was examined through scanning electron microscopy (NovaNano, FEI) and transmission electron microscope (TEM) (Tecnai F20, FEI). Porosity tests were calculated using Silwick (Porous Materials, Inc.) as the wetting liquid (surface tension: 20.1 dynes/cm). Samples with 2.5 cm diameters were cut and saturated with the wetting liquid. The weight of the sample before and after wetting was measured and used to determine the porosity.

2.2.2 Wettability

Contact angle tests were carried out at room temperature using an EasyDrop Standard drop shape analysis (KRUSS, Germany). A 2 μL droplet of deionized water was produced on the membrane surface and the digital image was used to determine contact angle. The contact angle was measured using sessile drop, tangent line and circle fitting methods and the average of these values was recorded.

2.2.3 Mechanical properties

The mechanical properties of CNS and NC/CNS membranes were investigated with Instron 5966 Dual Column Tabletop Testing System (Italy). Standard dog-bone specimens were cut out using the Ray-Ran Hand Operated Test Sample Cutting Press (UK). The material was stretched in tension at a strain rate of 1 mm/min and its response was recorded until failure. Stress–strain curves were generated from which elastic modulus, tensile strength and material ductility were studied.

2.2.4 Electrical properties

Electrical conductivity of the membrane was measured using a four point probe (LakeShore,

USA), according to the Van der Pauw method. Four electrodes were pasted on the membrane surface using silver paint dots. The electrodes were marked as 1–4 in clockwise direction. Current was passed through electrodes 1 & 2 and the potential was measured between 3 & 4 electrodes. Four consecutive measurements were carried out by applying a current between 2 & 3, 3 & 4, and 4 & 1 and measuring the potential between 4 & 1, 1 & 2 and 2 & 3 respectively.

2.2.5 Nanofiltration

NC-CNS membranes were tested to confirm they are nanofiltration membranes using aqueous solutions of calcium chloride and of magnesium sulfate to test the rejection of divalent anions. A feed concentration of 10,000 ppm was used for each solution in the in-lab membrane filtration unit shown in **Figure 1**. Fabricated membranes of diameter 8.5 cm were wetted before conducting filtration experiments. Testing was performed for 30 mL under a pressure of 10 bars.

Figure 1: Membrane filtration unit

No support layer was used except for the metal flange on which the membrane was secured in the membrane filtration unit. Permeate conductivity was measured by accumet® XL 50 dual channel pH/Ion/conductivity meter and the obtained value was converted to ppm total dissolved solids (TDS). Salt rejection rate (%SR) was measured using the following formula:

$$\%SR = \frac{C_{feed} - C_{permeate}}{C_{feed}},$$

where C_{feed} and $C_{permeate}$ are the concentrations (in ppm) of the feed and permeate respectively.

2.2.6 Electrochemical Measurements

Glassy carbon electrode coated with CNS and CNS-NC (referred to as GC-CNS and GC-CNS-NC in following text). Electrodes were prepared by dispersing 10 mg of CNS and CNS-NC in 1ml of 5wt% Nafion solution using a bath sonicator to obtain homogeneous suspension. The resulting suspension was coated on the GC and dried in an oven at 50 ^{o}C to obtain CNS or CNS-NC coated electrode.

Linear polarization studies were performed on Autolab302N potentiostat/galvanostat using GC (or GC coated with CNS and CNS-NC) as a working electrode, Pt wire as a counter electrode and Ag/AgCl (3.5M KCl solution) as a reference electrode. All the measured potentials were reference with respect to RHE by changing the Ag/AgCl electrode potential as (0.205 + 0.059 x pH) V. The working electrodeshave an area of1.11 cm^2. Before running the linear polarization scan, all the electrodes were run for ten cyclic voltammetry curves in the appropriate potential range depending on the HER/OER to stabilize the electrodes.

2.2.7 Contact angle measurement

Contact angle (θ) measurements were performed on an EASY DROP Contact Angle measurement instrument from Kruss (Hamburg, Germany) equipped with image-processing software. A piece of electrode was placed on a platform and deionized (DI) water was used as liquid at room temperature. A micro-syringe was then used to generate 3-4 μL of the droplets on the electrode surface. The instrument captures a digital image of the drop on the surface and estimates the θ by geometrical methods (sessile drop, circle-fitting, etc.). A minimum of three measurements were recorded for each surface.

3 Results and Discussion

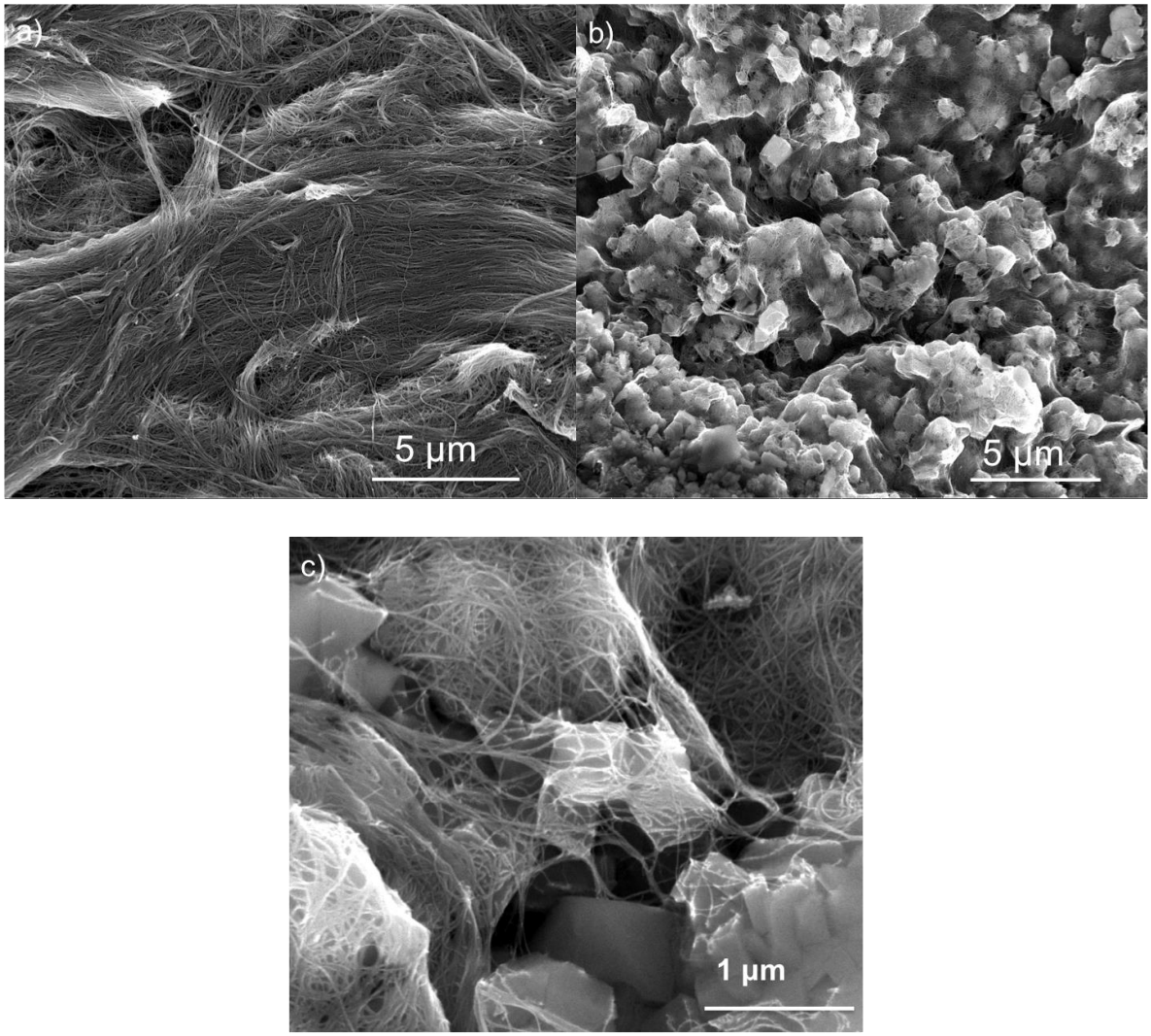

Figure 2: SEM images of a) CNS membrane, b) NC/CNS membrane and c) NC/CNS at high magnification

The morphology of CNS and NC/CNS membranes as characterized by SEM is shown in **Figure 2**. CNS is made up of a network of CNTs formed by branching and crosslinking of CNTs during chemical vapor deposition [13]. CNS membranes are characterized by a porous structure of randomly oriented CNTs. Sonication led to a well-dispersed network of CNTs, which is evident from the lack of CNT clusters or bundles (**Fig 2a**). The decrease in porosity due to the presence of NC was also measured (**Table 1**). CNS membranes are 45% porous, whereas NC/CNS

membranes have a significantly decreased porosity of 5%. This reduction in porosity can be attributed to the presence of NC, whose chains shrink together upon drying causing the material to densify.

Table 1: Porosity of membranes with and without NC

Membrane	Thickness (µm)	Porosity
CNS	120	45 ± 1
NC/CNS	80	5 ± 1

TEM images of dried CNS and NC/CNS suspensions are shown in **Figure 3**. The branched structure of CNS is visible in Figure 3a. The diameter of the CNTs is in the range of 5-10 nm, indicating no presence of aggregates and hence good dispersion of CNS in the suspension. When CNS was incorporated during NC preparation, a network of NC is shown to entrap the CNTs. This characteristic network structure of NC is a result of chains bonding together randomly upon regeneration, as has been previously observed [11].

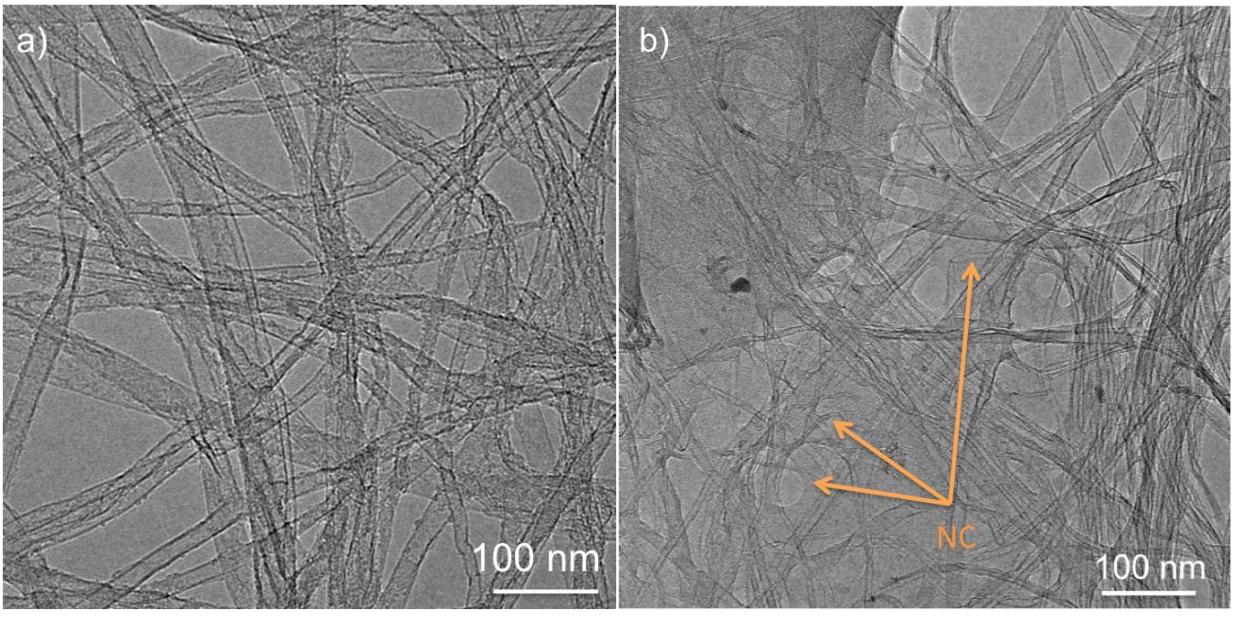

Figure 3: TEM images of a) CNS and b) NC/CNS suspension

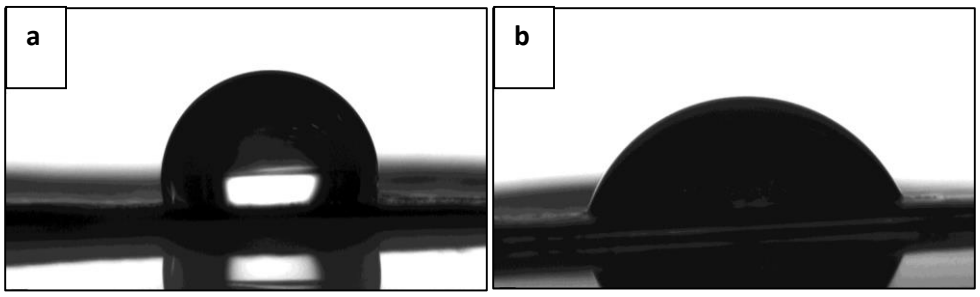

Figure 4: Water droplet on a) CNS and b) NC/CNS membrane

Contact angle measurements were carried out to study the effect of NC on the wettability of CNS membranes to water (**Figure 4**). It was found that CNS membranes had a static contact angle of about 105±3°, whereas the static contact angle for NC/CNS reduced to 73±3°. This enhancement of hydrophilicity is due to the more amorphous structure of networked cellulose [12], that can uphold moisture more readily. Improved hydrophilicity is considered an advantage for greater permeability and better resistance to fouling [15].

The mechanical behavior of CNS and NC/CNS membranes was also studied. Stress-strain curves are shown in **Figure 5**. NC/CNS membranes exhibit a tensile strength more than 10 times that of CNS membranes, increasing from 5 MPa to 54 MPa. This can be attributed to the compaction of the membrane and decrease in pore volume by addition of NC. Furthermore, elongation at break also increases slightly in NC/CNS (0.06 mm/mm) as compared to CNS membranes (0.04 mm/mm). Table 1 summarizes the mechanical properties values of the NC/CNS membranes.

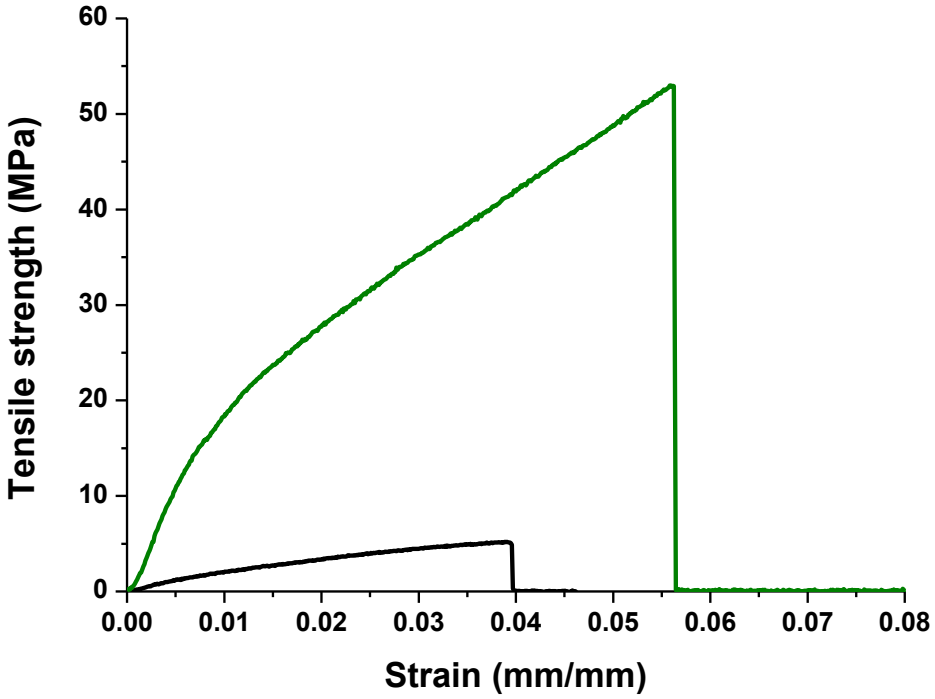

Figure 5: Stress–strain diagrams for CNS (black) and NC-CNS (green) membranes

The self-supporting NC/CNS membranes were then tested for nanofiltration of divalent ions using an aqueous solution of 20,000 ppm $CaCl_2$ as the feed. A pressure of 15 bars was applied across the membrane. **Table 2** shows the performance parameters of the two membranes. Because of its highly porous structure, the salt permeation through the membrane was 100%. However, the NC/CNS membrane was able to reject Ca^{2+} salts with a rate of 47%. This significant hike in salt rejection rate can be attributed to the smaller pores and better permeability of water through the membrane, as a result of NC. Additionally, $MgSO_4$ rejection was much higher at 60%, illustrating the use of these membranes for nanofiltration of divalent cations and anions. NC has previously been used in RO membranes in which the principle mode of transport is via diffusion through the membrane [12]. In nanofiltration, both sieving and diffusion mechanisms play a role in transport through the membrane[16]. It is likely that the presence of 50 wt. % NC encapsulating CNS

enhances transport by diffusion. It is likely that the low selectivity of 47% is due to the smaller Cl^- anions. Rejection for $MgSO_4$ also needs to be further improved for these membranes to compete with commercial nanofiltration membranes. However, it has been demonstrated that conductive NC/CNS membranes with high electrical conductivity may be tuned to nanofiltration, allowing them to be used for electrochemical self-cleaning, as previously demonstrated by our group. Although the conductivity of the membrane reduced slightly due to the insulating nature of cellulose, the membrane is still highly conductive with a conductivity value of 2200 S/m. This high electrical conductivity is essential in the periodic self-cleaning of membranes using periodic electrolysis as shown elsewhere [17].

Table 2: Performance parameters of CNS and NC/CNS membranes

Membrane	Conductivity (S/cm)	Feed (ppm)	Salt rejection (%)	Flux (L m^{-2} h^{-1})
CNS	35	10,000	0	-
NC/CNS	22	10,000 $CaCl_2$	47 ± 2	99
NC/CNS	22	10,000 $MgSO_4$	60 ± 2	120

The permeate flux of the membrane is comparable to commercial nanofiltration membranes from Amfor, Inc. (China), whose manufacturers report a permeate flux of 100 L m^{-2} h^{-1} for the same transmembrane pressure [18].

Electrocatalytic activity of the CNS and CNS-NC membranes were evaluated in acidic and basic media. **Figure 6a** shows the polarization curves of Pt, glassy carbon (GC), GC coated with CNS (GC-CNS) and GC coated with NC/CNS (GC_CNS-NC) for hydrogen evolution reaction (HER) in 0.5 M H_2SO_4 at a scan rate of 50 mV/sec. Onset potential of hydrogen evolution reaction were calculated at a current density of 1 mA/cm^2. For standard Pt electrode, onset potential

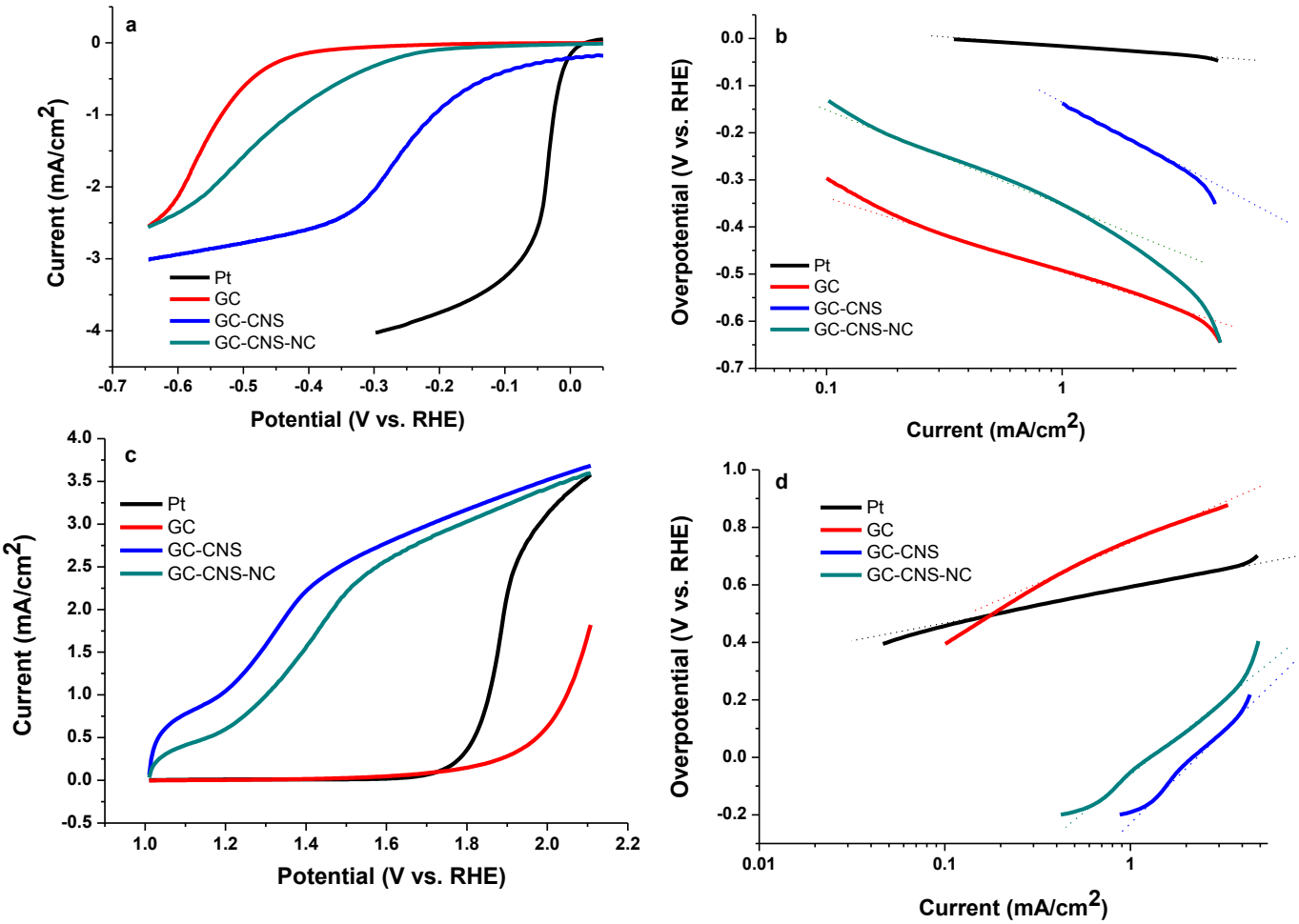
a
Current (mA/cm2)
Potential (V vs. RHE)
Pt
GC
GC-CNS
GC-CNS-NC
b
Overpotential (V vs. RHE)
Current (mA/cm2)
c
d

Figure 6. Linear polarization curves (a,c) and Tafel plots (b,d) of different electrodes for hydrogen evolution and oxygen generation in 0.5M H_2SO_4 respectively.

located at -17 mV with reference to RHE electrode potential. Onset potentials for GC, GC-CNS and GC-CNS-NC electrode were found to be -492 mV, -137 mV and -353 mV respectively. GC-CNS-NC showed higher overpotential for HER as compared to GC-CNS electrode, this may be due to the inactivity of the NC. However, when the mass activity was calculated for the electrode material, it was found that GC-CNS-NC produces 400 mA/ g compared to 204 mA/g for GC-CNS electrodes at overpotential of -353mV and -137mV respectively. This improved mass density could be correlated with the hydrophilicity of the electrode imparted by the NC. The kinetics of HER were studied using the Tafel equation, η = a + b log j, where η **is** overpotential, b is Tafel slope and j is a current density. Tafel slope calculated from Figure 6b are 30, 150, 268, and 315 mV/dec for Pt, GC, GC-CNS and GC-CNS-NC respectively.

Linear polarization curves correspond to oxygen evolution reaction (OER) for Pt, glassy carbon (GC), GC-CNS and GC_CNS-NC in 0.5 M H_2SO_4 at a scan rate of 50 mV/sec are shown in Figure 6c and calculated Tafel slopes are shown in Figure 6d. Onset potentials for oxygen generation are 1.82, 1.98, 1.04 and 1.18 V for Pt, GC, GC-CNS and GC-CNS-NC respectively. A significant reduction in the onset potential for OER was found for GC-CNS and GC-CNS-NC electrodes as compared to standard Pt electrode.

Overpotentials for OER were calculated as η = onset potential (vs. RHE) – 1.23 V for different electrode materials. Tafel slopes were found to be 131, 288, 557 and 483 mV/dec for Pt, GC, GC-CNS and GC-CNS-NC respectively.

Linear polarization curves for HER in 0.1M KOH for Pt, GC, GC-CNS and GC-CNS-NC are shown in Figure 7a. Onset potential of HER for standard platinum electrode was found to be -5mV. Onset potential required to drive current density of 1mA/cm2 are -709, 26 and 34 mV for GC, GC-CNS and GC-CNS-NC electrodes respectively. It is worth noting that the overpotential required for HER in basic media for GC-CNS and GC-CNS-NC are lower compared to in the acidic medium.

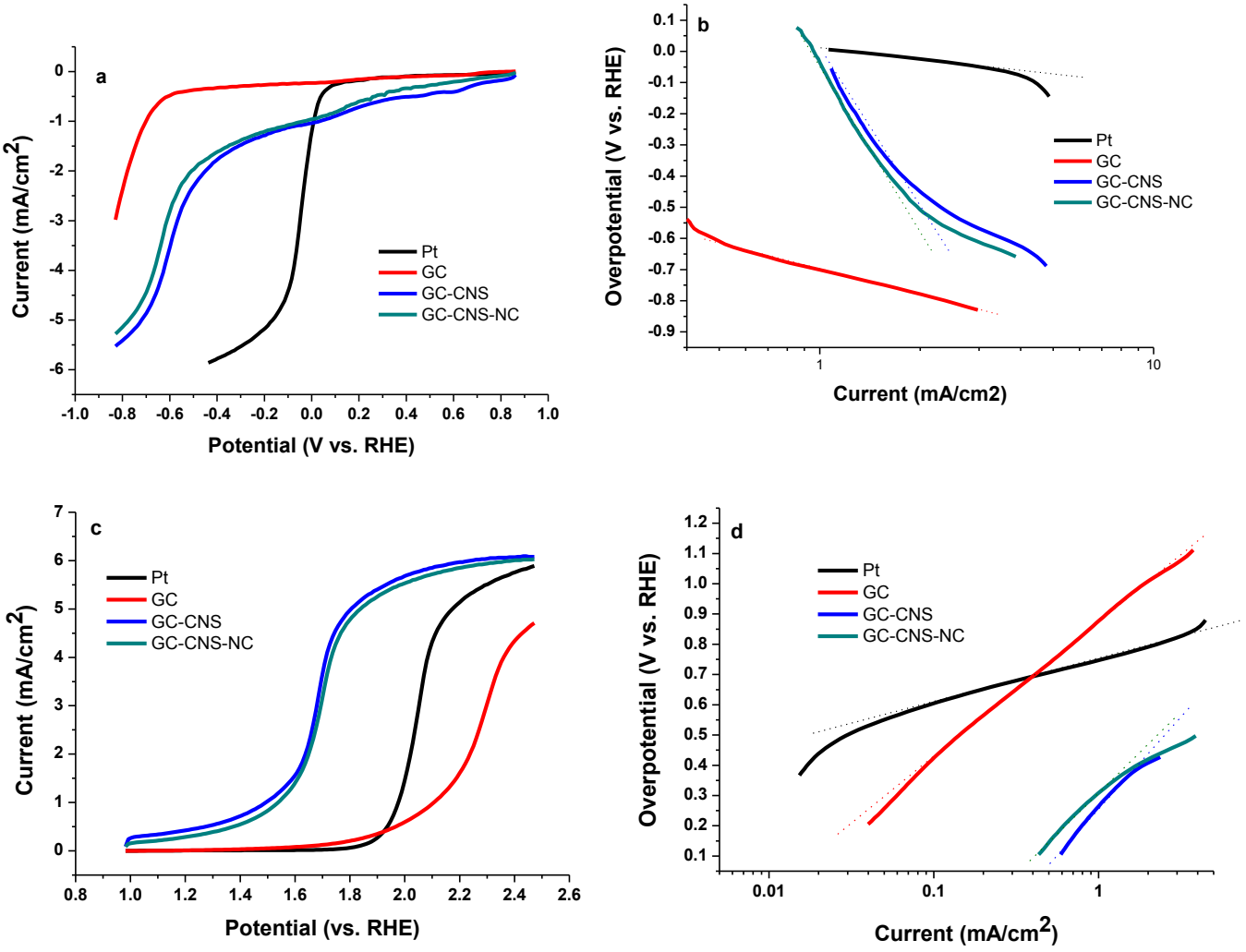

Figure 7. Linear polarization curves (a,c) and Tafel plots (b,d) of different electrodes for hydrogen evolution and oxygen generation reaction in 0.1M KOH respectively.

Tafel slopes calculated for HER are shown in Figure 7b; Pt, GC-, GC-CNS and GC-CNS-NC has Tafel slope of 106, 259, 460 and 417 mV/dec respectively. Figure 7c showed the linear polarization curves for different electrodes in basic media. An OER overpotential of 749 mV and 880 mV required for Pt and GC electrodes. Coating of CNS and CNS-NC on the GC electrode significantly reduces the overpotential to 1.1 mV for both electrodes. The corresponding Tafel slopes for electrodes are shown in Figure 7d.

During the electrolysis process at the electrode/electrolyte interface, gas bubbles forms on the surface the electrode and starts moving up and then leave the surface when size become appropriate. The long stay of gas bubble on the surface reduces the charge transfer reaction at the interface and hence reduces the efficiency of the electrolysis process. To reduce the resistance due to gas bubble, hydrophilic electrode surface plays an important role. CNS are hydrophobic in nature having static contact angle of ~ 105±3^{o}. Static contact angle of 65±3^{o} was measured for CNS-NC electrode surface. Networked cellulose has hydrophilic nature and NC/CNS composites have improved hydrophilicity which favors quick regeneration of the electrode surface during electrolysis process.

Optical images of the evolution of hydrogen gas bubbles on the surface of CNS and CNS-NC are shown in Figure 8. Figure 8a and 8c were captured when the hydrogen evolution just started on the CNS and CNS-NC surface respectively. Figure 8b and 8d, when the hydrogen gas evolves contiuously on the CNS and CNS-NC surface respectively. Figure 8a and 8b showed that bubbles

start growing and then leave the CNS surface after achieveing a big bubble size. On the other hand, if one compares Figure 8c and 8d with 8a and 8b, it is evident that the gas bubble size is comparatively smaller on the CNS-NC surface. This is due to hydrophillic nature of the CNS-NC electrode surface which assists the regeneration of the electrode surface for evolution of the gases.

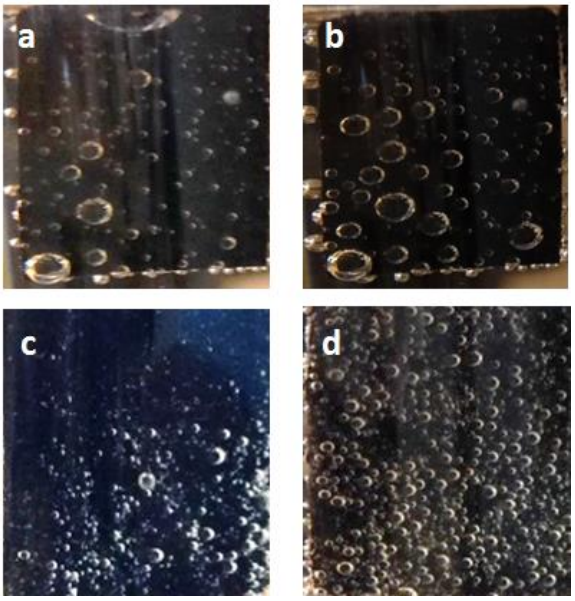

Figure 6. Optical images of hydrogen evolution on the CNS membrane (a, b) and CNS-NC membrane surface (c, d).

3. Conclusion

In this work, the pore size and wettability of electrically conductive CNS membranes were controlled with a form of networked cellulose. Use of cellulose led to increased hydrophilicity and lower porosity, allowing selective filtration of divalent ions such as Ca^{2+}, Cl^{-}, Mg^{2+} and SO_4^{2-}. NC/CNS membranes also demonstrated strength more than 10 times higher than that of CNS membranes, due to the closely bonded networked structure of NC that entrapped the randomly

oriented CNS. Despite the insulating nature of cellulose, NC/CNS membranes with 50 wt, % NC still retained excellent electrical conductivity while enabling the nanofiltration of $MgSO_4$ with a rejection rate of 60%. The high flux of these membranes also renders them suitable as pretreatment of RO. Future work includes enhancing the rejection rate through using other additives. Due to their high electrical conductivity, these membranes may be beneficial in the mitigation of fouling through electrical methods, as previously demonstrated for CNS microfiltration membranes. It was shown that NC aided the regeneration of the membrane surface during electrolysis, due to enhanced hydrophilicity. It was also shown that onset potential for oxygen generation was significantly lower in CNS-based electrodes than for Pt. Although CNS-NC exhibited a higher overpotential than CNS for HER due to the non-conducting nature of cellulose, it had a higher mass activity. Ideally, high mass activity at low overpotentials is desirable for electrode materials and further improvements can be made to use CNS as an elctroactive material without compromising its electrocatalytic properties.

Acknowledgement

The authors would like to thank Lockheed Martin for providing the CNS material and partially funding this work.

References

1. Vecitis, C.D., et al., *Electrochemical Multiwalled Carbon Nanotube Filter for Viral and Bacterial Removal and Inactivation.* Environmental Science & Technology, 2011. **45**(8): p. 3672-3679.
2. Rahaman, M.S., C.D. Vecitis, and M. Elimelech, *Electrochemical Carbon-Nanotube Filter Performance toward Virus Removal and Inactivation in the Presence of Natural Organic Matter.* Environmental Science & Technology, 2011. **46**(3): p. 1556-1564.
3. Hashaikeh, R., B. Lalia, and N. Hilal, *Novel in-situ membrane cleaning using periodic electrolysis*. 2014, Google Patents.

4. Lalia, B.S., et al., *Electrically conductive membranes based on carbon nanostructures for self-cleaning of biofouling.* Desalination, 2015. **360**: p. 8-12.
5. Ahmed, F., et al., *Electrically conductive polymeric membranes for fouling prevention and detection: A review.* Desalination, 2016.
6. Duan, W., et al., *Electrochemical mineral scale prevention and removal on electrically conducting carbon nanotube - polyamide reverse osmosis membranes.* Environmental Science: Processes & Impacts, 2014. **16**(6): p. 1300-1308.
7. Dudchenko, A.V., et al., *Organic fouling inhibition on electrically conducting carbon nanotube–polyvinyl alcohol composite ultrafiltration membranes.* Journal of Membrane Science, 2014. **468**(0): p. 1-10.
8. de Lannoy, C.-F., et al., *Aquatic Biofouling Prevention by Electrically Charged Nanocomposite Polymer Thin Film Membranes.* Environmental Science & Technology, 2013. **47**(6): p. 2760-2768.
9. de Lannoy, C.F., et al., *A highly electrically conductive polymer–multiwalled carbon nanotube nanocomposite membrane.* Journal of Membrane Science, 2012. **415–416**(0): p. 718-724.
10. Simon, A., et al., *Effects of caustic cleaning on pore size of nanofiltration membranes and their rejection of trace organic chemicals.* Journal of Membrane Science, 2013. **447**: p. 153-162.
11. Hashaikeh, R. and H. Abushammala, *Acid mediated networked cellulose: Preparation and characterization.* Carbohydrate polymers, 2011. **83**(3): p. 1088-1094.
12. Anis, S.F., B.S. Lalia, and R. Hashaikeh, *Controlling swelling behavior of poly (vinyl) alcohol via networked cellulose and its application as a reverse osmosis membrane.* Desalination, 2014. **336**(0): p. 138-145.
13. Shah, T.K., et al., *Carbon nanostructures and methods of making the same*. 2013, Google Patents.
14. Shah, T.K., et al., *Carbon nanostructures and methods for making the same*. 2014, Google Patents.
15. Li, M., et al., *Highly hydrophilic and anti-fouling cellulose thin film composite membrane based on the hierarchical poly(vinyl alcohol-co-ethylene) nanofiber substrate.* Cellulose, 2015. **22**(4): p. 2717-2727.
16. Mulder, J., *Basic principles of membrane technology*. 2012: Springer Science & Business Media.
17. Hashaikeh, R., et al., *A novel in situ membrane cleaning method using periodic electrolysis.* Journal of Membrane Science, 2014. **471**(0): p. 149-154.
18. Abuhabib, A., *Modified Nanofiltration Membranes Performance Improvement for Desalination Applications.* 2015.